

## PDF hosted at the Radboud Repository of the Radboud University Nijmegen

The following full text is a publisher's version.

For additional information about this publication click this link.

<http://hdl.handle.net/2066/34714>

Please be advised that this information was generated on 2019-04-25 and may be subject to change.

*Baltic Astronomy, vol. 15, 259–268, 2006.*

## ULTRACAM PHOTOMETRY OF PULSATING SUBDWARF B STARS

C. S. Jeffery<sup>1</sup>, C. Aerts<sup>2,3</sup>, V. S. Dhillon<sup>4</sup> and T. R. Marsh<sup>5</sup>

<sup>1</sup> *Armagh Observatory, College Hill, Armagh BT61 9DG, U.K.*

<sup>2</sup> *Institute of Astronomy, Catholic University of Leuven, Celestijnenlaan 200 B, B-3001 Leuven, Belgium*

<sup>3</sup> *Department of Astrophysics, Radboud University Nijmegen, PO Box 9010, 6500 GL Nijmegen, The Netherlands*

<sup>4</sup> *Department of Physics and Astronomy, University of Sheffield, Sheffield S3 7RH, U.K.*

<sup>5</sup> *Department of Physics, University of Warwick, Coventry CV4 7AL, U.K.*

Received 2005 September 29

**Abstract.** High-speed multicolor photometry with ULTRACAM promises to revolutionize the study of pulsating subdwarf B stars. As well as providing high  $S/N$  light curves with excellent temporal resolution, color amplitude ratios may be used to discriminate between different pulsation modes. In this paper we review the methods for mode determination developed for KPD 2109+4401 and HS 0039+4302 since the 2003 workshop. We also present a new dataset obtained over 6 nights in 2004 August for PG 0014+067. This was the first sdB star to be subjected to a detailed asteroseismological analysis. It was also the subject of the WET campaign in 2004 October/November (XCov24). We discuss the implications of our new observations for mode identification and rotation.

**Key words:** stars: hot subdwarfs – stars: oscillations

### 1. INTRODUCTION

The discovery of pulsations in subdwarf B (sdB) stars has provided a vital key for measuring their global properties and for exploring their internal structure. Such information allows us to test theories of stellar physics, the structure of horizontal-branch stars and the origin of sdB stars. Many aspects of sdB star astronomy are described elsewhere in this volume; here we describe our application of high-speed multicolor photometry to the asteroseismology of sdB stars.

### 2. NON-RADIAL OSCILLATIONS

Nonradial oscillations (*nro*'s) are waves travelling through the interior of a star. They may manifest as surface displacements characterized by a spherical harmonic:

$$\xi = \sum_{l,m} Y_{lm}(\theta, \phi) \cos(\omega t) \quad (1)$$

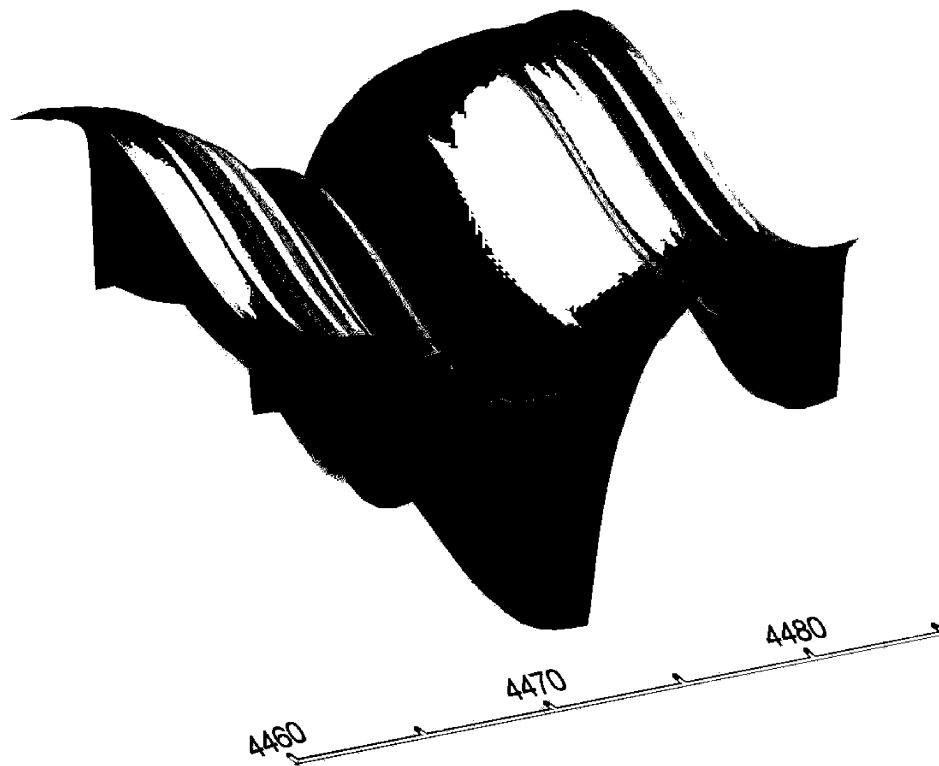


**Fig. 1.** Spectral variation near HeI 4471 Å due to one cycle of a radial mode ( $\ell, m = 0, 0$ ) in a pulsating sdB star. Scales are arbitrary.

where  $\nu$  represents the frequency of the oscillation,  $\ell$ : the degree of the spherical harmonic or the number of lines of nodes on a spherical surface and  $m$ : the azimuthal number or the number of lines of nodes passing through the polar axis ( $|m| \leq \ell$ ). Besides these surface nodal line identifications,  $n$  (or  $k$ ) denotes the order of the oscillation eigenfunction. In the linear adiabatic approximation this is equivalent to the number of nodes along the radial direction.

Such oscillations are probably excited at some level in a very large fraction of all stars. Many hundreds of modes have been identified in the Sun. However, because of superposition and cancellation, *nro*'s are generally manifest only when they are both of sufficiently low degree *and* of significant amplitude. They become observable principally as variations in total light, color, radial velocity or absorption line profile. The effects of low-degree oscillations on a stellar spectrum are illustrated in Figures 1 and 2. Fig. 1 shows the flux as a function of wavelength and time through one cycle of a radial pulsation with a simulated velocity amplitude of  $10 \text{ km s}^{-1}$ . The top panel in Fig. 2 shows the average spectrum of a star in the region of  $\text{H}\gamma$ . Below are shown grey-scale representations of residual time series (e.g., the average spectrum subtracted from the time-varying spectrum) for three non-radial modes (amplitudes =  $10 \text{ km s}^{-1}$ ). The horizontal shading shows how the total flux varies through the pulsation cycle. The s-waves running through the vertical bands demonstrate how the disk-averaged radial motion of the stellar surface modifies the profiles of the absorption lines.

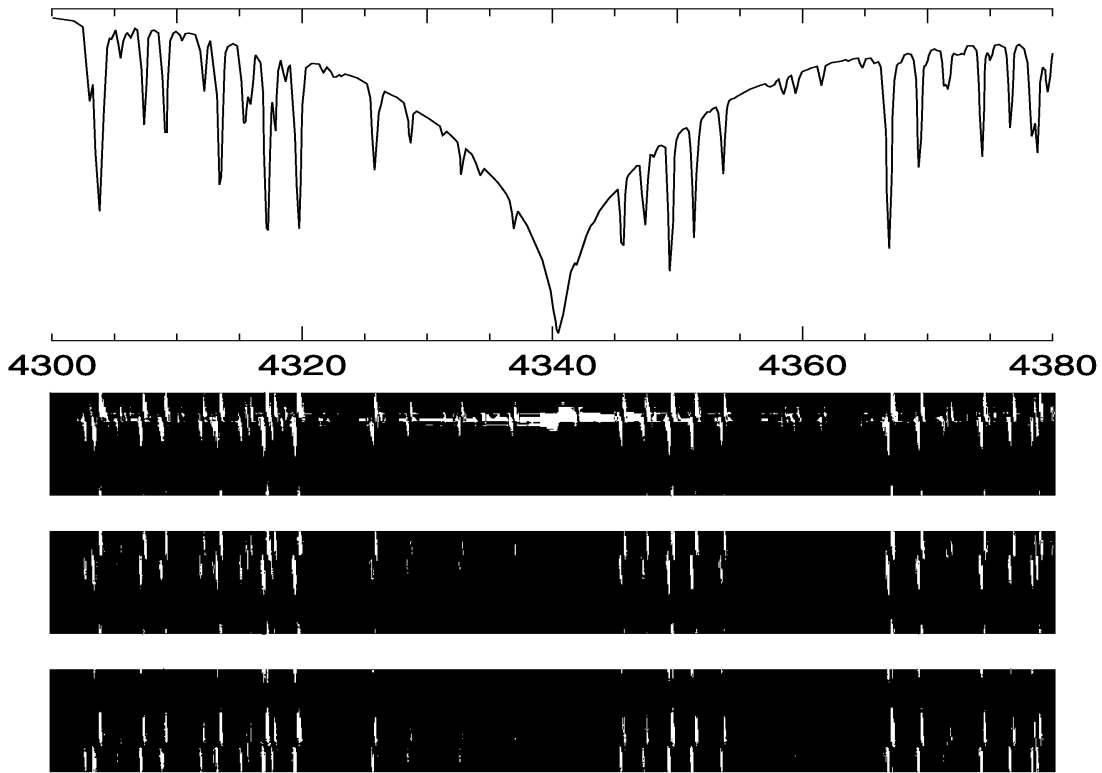


**Fig. 2.** Mean and trailed residual spectra for modes  $\ell, m = (0,0), (2,0)$  and  $(2,2)$  (top to bottom).

Because *nro*'s propagate through the stellar interior, they provide indirect information about stellar structure. The best example is provided by the Sun, where *nro*'s have been used to measure the internal density profile, internal rotation speed, structure of the tachocline, and the presence of sunspots on the invisible hemisphere. In stars, internal structure is inferred by finding the best match between observed oscillation frequencies and frequencies computed from families of stellar interior models. Generally, only frequencies are used, principally because these can be measured from a single-channel light curve. In the best cases, such methods may yield  $n$  from the frequencies if the stellar radius is known and  $m$  from frequency splitting if rotation lifts the azimuthal degeneracy.  $\ell$  is harder to identify, but can generally be assumed to be small.

We have attempted various approaches to identify  $\ell$  in the *nro*'s of pulsating *sdB* stars. One result is particularly apposite (Heynderickx et al. 1994). For a given mode, the ratio of photometric amplitude at different wavelengths is independent of the inclination of the pulsation axis  $i$  to the observer *and* to  $m$ , but is sensitive to  $\ell$ . In principal, this allows us to identify  $\ell$  from multicolor photometry or spectrophotometry, and thereafter by elimination to identify  $n$ . With  $n$  and  $\ell$  derived empirically, the comparison with theoretical models is much more tightly constrained. We may also be able to learn something about rotation by identifying multiplets, i.e., oscillations at different frequencies with the same  $n, \ell$  but different  $m$ .

We have therefore obtained high-speed multicolor photometry for a number of *sdB* stars using 4 m telescopes and developed the necessary diagnostic tools in an effort to identify  $n$  and  $\ell$  for comparison with models.

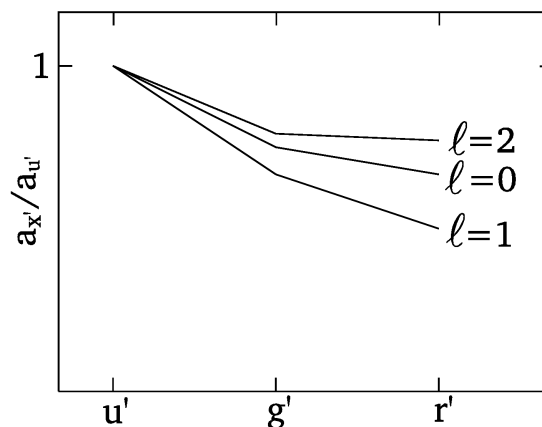
**Table 1.** Codes for spectroscopy and photometry simulations.

STERNE: LTE line-blanketed model atmospheres IN: $T_{\text{eff}} = 25 - 35$ kK, $\log g = 4 - 6$ , $X_i$ OUT: model grid: $T_\tau, P_\tau$
SPECTRUM: LTE specific intensities IN: STERNE models, $X_i, v_{\text{turb}}, \langle \mu \rangle, \langle \lambda \rangle$ OUT: intensity grid: $I_{\mu\lambda}$
BRUCE: surface description of <i>nro</i> 's IN: $M, T_{\text{eff}}, R_{\text{eq}}, i, v_{\text{rot}}, \langle \ell, m, P, v \rangle, n_t, t_n$ OUT: $T_{\theta\phi}, g_{\theta\phi}, \mu_{\theta\phi}, a_{\theta\phi} \sin i, v_{\theta\phi} \sin i$
KYLIE: apparent fluxes IN: BRUCE models, $I_{\mu\lambda}, \langle \lambda \rangle, \delta\lambda$ OUT: $F_{\lambda t}$
FAST: Fourier analysis of spectroscopic time-series IN: $F_{\lambda t}$ OUT: $\nu, \phi, a$

### 3. THEORETICAL PHOTOMETRY

The color-amplitude ratio method involves measuring the amplitude  $a$  of an oscillation in light measured in two or more wavelength intervals. The principle is illustrated schematically in Figure 3. In order to determine the value of  $\ell$  responsible for an observed curve in this figure, it is first necessary to derive theoretical amplitude ratios from model atmospheres and pulsation theory. For consistency we will refer to the pass bands  $u'$ ,  $g'$  and  $r'$  of the Sloan Digital Sky Survey (Fukugita et al. 1996). A summary of the codes used, with their principal inputs and outputs, is given in Table 1. The same codes, models and methods may of course be used to compute amplitude ratios for broad-band photometry and for spectrophotometry, as well as for detailed modelling of line-profile and radial velocity variations (cf., Figures 1 and 2).

Ramachandran et al. (2004) have predicted amplitude ratios for examples of both short and long-period sdBVs (EC 14026-2647 or V 361 Hya and PG 1716+426 variables). These are based on a grid of LTE model atmospheres and synthetic spectra computed (using programs STERNE and SPECTRUM) over a range of effective temperatures  $T_{\text{eff}}$ , surface gravities  $g$  and wavelengths  $\lambda$ , with appropriate values for composition  $X_i$  and microturbulent velocity  $v_{\text{turb}}$  (Jeffery et al. 2001). We calculate intensity spectra  $I_\nu$  including continuous intensities over a range

**Fig. 3.** Schematic amplitude ratios.

of cosine angles  $\mu$  in order to have an explicit description of what is known as the effective “limb darkening” at all wavelengths and, notably, in all lines.

Using program KYLIE (Townsend 1997), these intensity spectra are folded into a description of the moving surface provided by program BRUCE (ibid.), which calculates the surface geometry due to an adiabatic non-radial pulsation. This description includes the local  $T_{\text{eff}}$ ,  $g$ , projected velocity, surface area and inclination on a finely spaced grid covering the visible hemisphere.

The result is a time series of spectra, both line and continuum fluxes  $F_{\lambda t}$ ,  $F_{c\lambda t}$  for any specified temporal resolution and duration and for any desired spectral resolution and range, for a star pulsating in one or more non-radial modes, each with a specified period and amplitude.

This time series may be analyzed in a number of ways. For application of the amplitude ratio method, we convolved each spectrum  $F_{\lambda t}$  with photometric filter transmission functions (SDSS  $u'g'r'$  and Johnson  $UBVRI$ ) and converted to magnitudes. We then fitted one or more sine functions to determine the amplitude (and phase) of each oscillation in each filter ( $a_{u'}$ ,  $a_{g'}$ ,  $a_{r'}$ ) from which ratios were trivial to compute.

To find disk integrated and projected velocity amplitudes and line profile behavior, we identified a template spectrum  $A_{\lambda 0} - 1$  and computed the cross-correlation function (ccf) for each residual spectrum  $A_{\lambda t} - 1$ . The projected radial velocity  $v_t$  is measured by locating the peak of each ccf; higher order moments of the ccf are also computed. Sine functions are again fitted to each oscillation in order to measure amplitudes and phases. This work is done with the program FAST (Fourier Analysis of Spectroscopic Time Series).

This procedure may be further refined by choosing the wavelength region to include either a single line profile, many absorption lines or the entire UV/optical spectrum. Our goal is to choose a series of procedures which effectively mimic the observations as closely as possible.

#### 4. ULTRACAM PHOTOMETRY

ULTRACAM is a high-speed 3-channel CCD camera (Dhillon & Marsh 2001, Figures 4 and 5). Dichroics split the light into ultraviolet, visual and red wavebands which are simultaneously imaged with frame transfer CCDs, each having a  $5' \times 5'$  ( $1024 \times 1024$  pixels) imaging area. These CCDs use a masked area into which exposures are shunted rapidly from the imaging area, and which can then be read out while the next exposure is running. Mounted on the 4.2 m William Herschel Telescope, the combination of high throughput and high time resolution provides

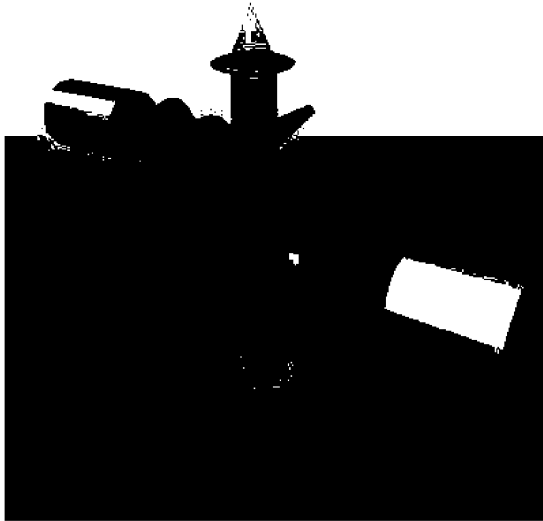


**Fig. 4.** ULTRACAM design.

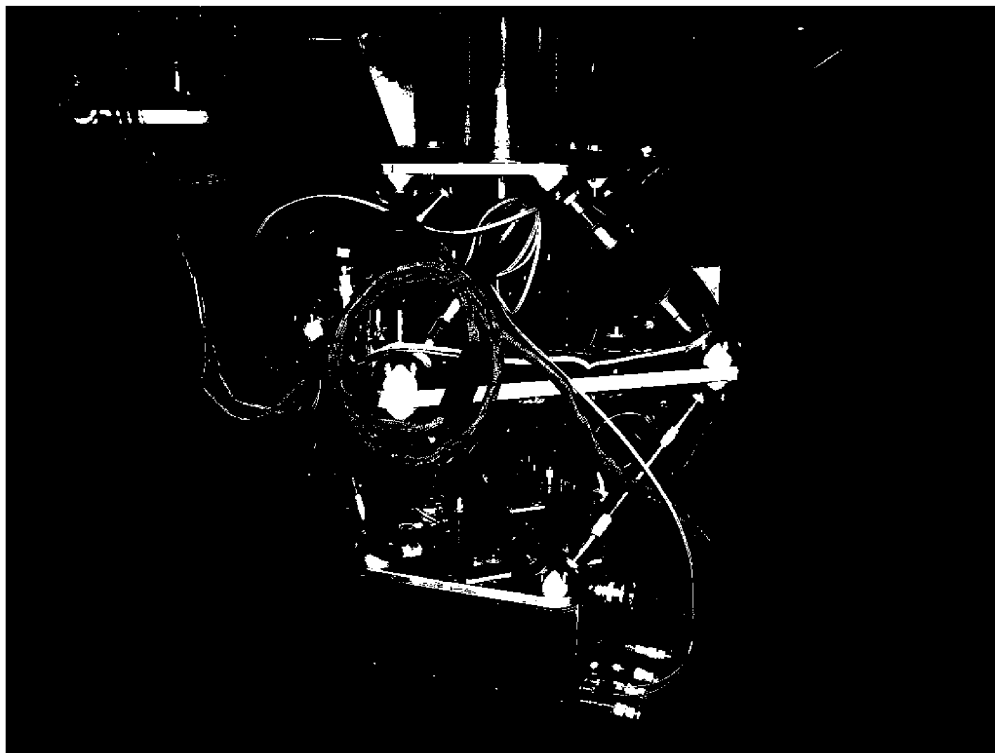


**Fig. 5.** ULTRACAM on the WHT.

an outstanding tool with which to explore pulsating sdB stars. It is equipped with filters  $u'$ ,  $g'$ ,  $r'$ ,  $i'$  and  $z'$  in the system designed for the Sloan Digital Sky survey (Fukugita et al. 1996), where the  $r'$ ,  $i'$  and  $z'$  may be interchanged in the red channel. By a judicious choice of windows on the CCD, frame rates of  $\sim 10^3$  Hz can be achieved. In our observations of sdBVs, frame rates of 0.1–10 Hz are more typical, primarily dictated by the pulsation frequencies 5 – 8 mHz and, for the brightest targets, the need to avoid CCD saturation.

#### 4.1. 2002 WHT campaign

First observations were obtained in 2002 September for the targets KPD 2109+4401 and HS 0039+4302. A portion of the light curves for each of these targets is shown in Figure 6. From amplitude spectra obtained with these light curves, the amplitudes of several modes were measured in each of the three ULTRACAM channels, being  $u'$ ,  $g'$  and  $r'$  of the SDSS system. The ratios  $a_{g'}/a_{u'}$  and  $a_{r'}/a_{u'}$  were computed and are shown in Figure 7. Meanwhile, theoretical models of the color amplitude ratios expected for non-radial oscillations of different spherical degree in sdBVs were computed by Ramachandran et al. (2004).

From Figure 7 it was clear that at least one oscillation in each target had to be a relatively high-degree ( $\ell = 4$ ) mode. Predicted ratios for low-degree modes ( $\ell = 0, 1, 2$ ) lie close together, so it is not possible to identify the degree of the observed modes so easily. There were no modes identified with  $\ell = 3$ . Assuming the observed frequencies belong to modes with unique  $k, \ell$  values (i.e., there is no rotational splitting), an additional constraint can be used. For a given degree  $\ell$ , modes of successive radial order  $k$  must be well-spaced in frequency, so modes of similar frequency cannot have the same  $\ell$ . By imposing such a constraint and

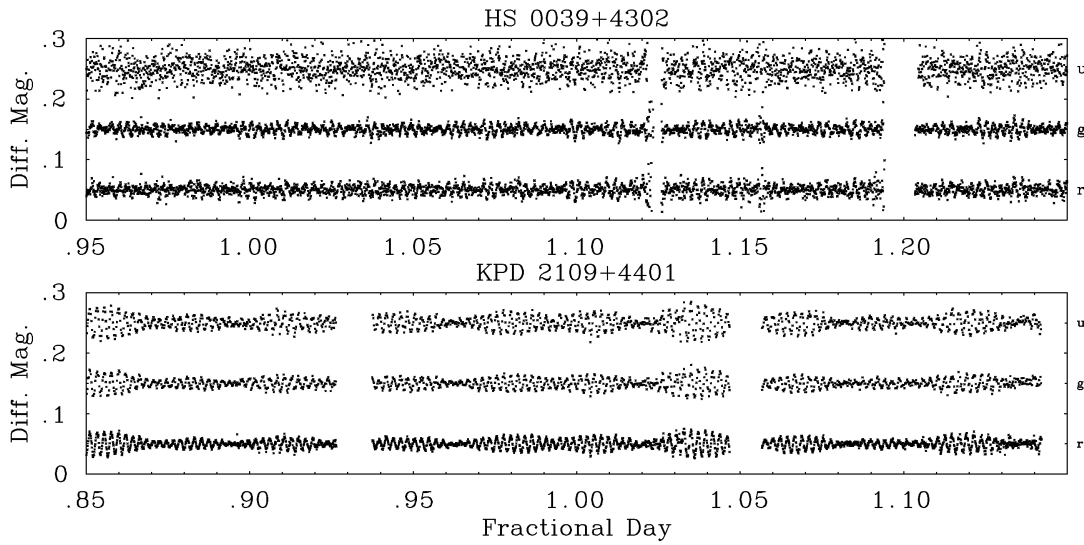


**Fig. 6.** Partial ULTRACAM light curves in  $u'$ ,  $g'$  and  $r'$  for *sdBVs* KPD 2109+4401 and HS 0039+3202 (adapted from Jeffery et al. 2004). Gaps are due to clouds.

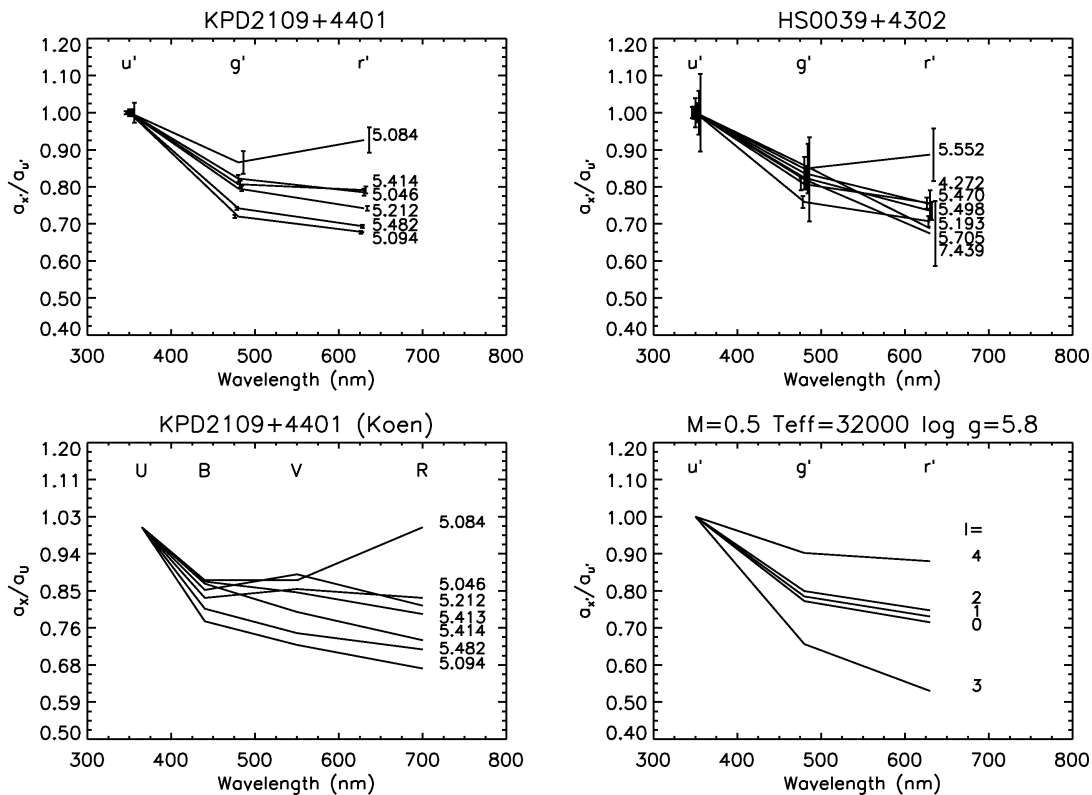


**Fig. 7.** Observed amplitude ratios for KPD 2109+4401 and HS 0039+4302 (top). Modes with  $a_{u'} < 1.4$  mmag shown as dashed lines. Lower panels show previous photometry of KPD 2109+4401 (left, Koen 1998) and a set of theoretical color-amplitude ratios  $\ell = 0, \dots, 4$  (right, Ramachandran et al. 2004). From Jeffery et al. (2004).



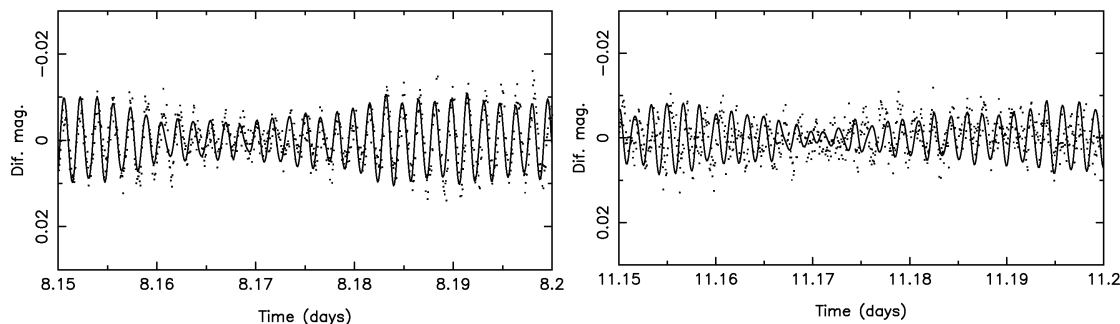


**Fig. 8.** Two sections of the white light curve of PG 0014+067 together with the 19-frequency solution. Time ( $t$ ) is JD-2453230. From Jeffery et al. (2005).

by comparing the color-amplitude ratios, it is possible to assign  $k$  and  $\ell$  values with some confidence. It is then possible to compare the observed frequency spectrum with theoretical models for non-radial oscillations in extended horizontal-branch stars (cf. Charpinet et al. 2002), and hence to select which models best represent the star observed in terms of total mass, envelope mass, age and other characteristics. A full description of the observations and the identification of the modes in these two stars is given by Jeffery et al. (2004).

#### 4.2. 2004 WHT campaign

A second ULTRACAM run to observe pulsating sdBVs was executed in 2004 September. Observations of a secondary target, the 17th mag sdB SDSS J 171722.08 +58055.8, are presented by Aerts et al. (2006).

The primary target was the magnitude 16.5 star PG 0014+067, previously the subject of successful asteroseismological studies by Brassard et al. (2001) and Charpinet et al. (2005). This star showed  $\sim 20$  independent frequencies in its white light curve with frequencies between 5.7 and 12.9 mHz. Our aim was to check mode identifications deduced from the theoretical model that best fitted the frequency spectrum, and also to support a subsequent Whole Earth Telescope

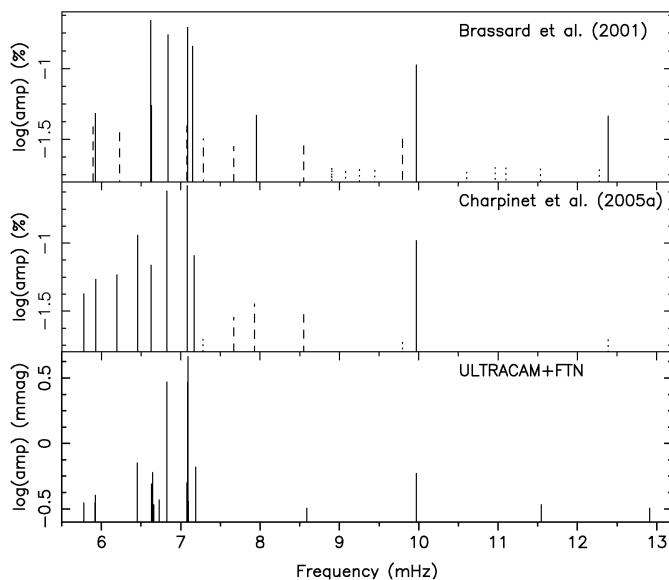


**Fig. 9.** Comparison of three independent frequency amplitude spectra for PG 0014+067. Solid lines are  $4\sigma$  detections, dashed lines  $3\sigma$ , and dotted lines are observed frequencies coincident with frequencies in best fit models. From Jeffery et al. (2005).

campaign to improve the overall frequency resolution. Although a much more challenging target than the 2002 targets, it was possible to observe this object with the WHT for  $\sim 6$  hours on each of 6 successive nights. These observations were supported with data from Faulkes Telescope North, located on the

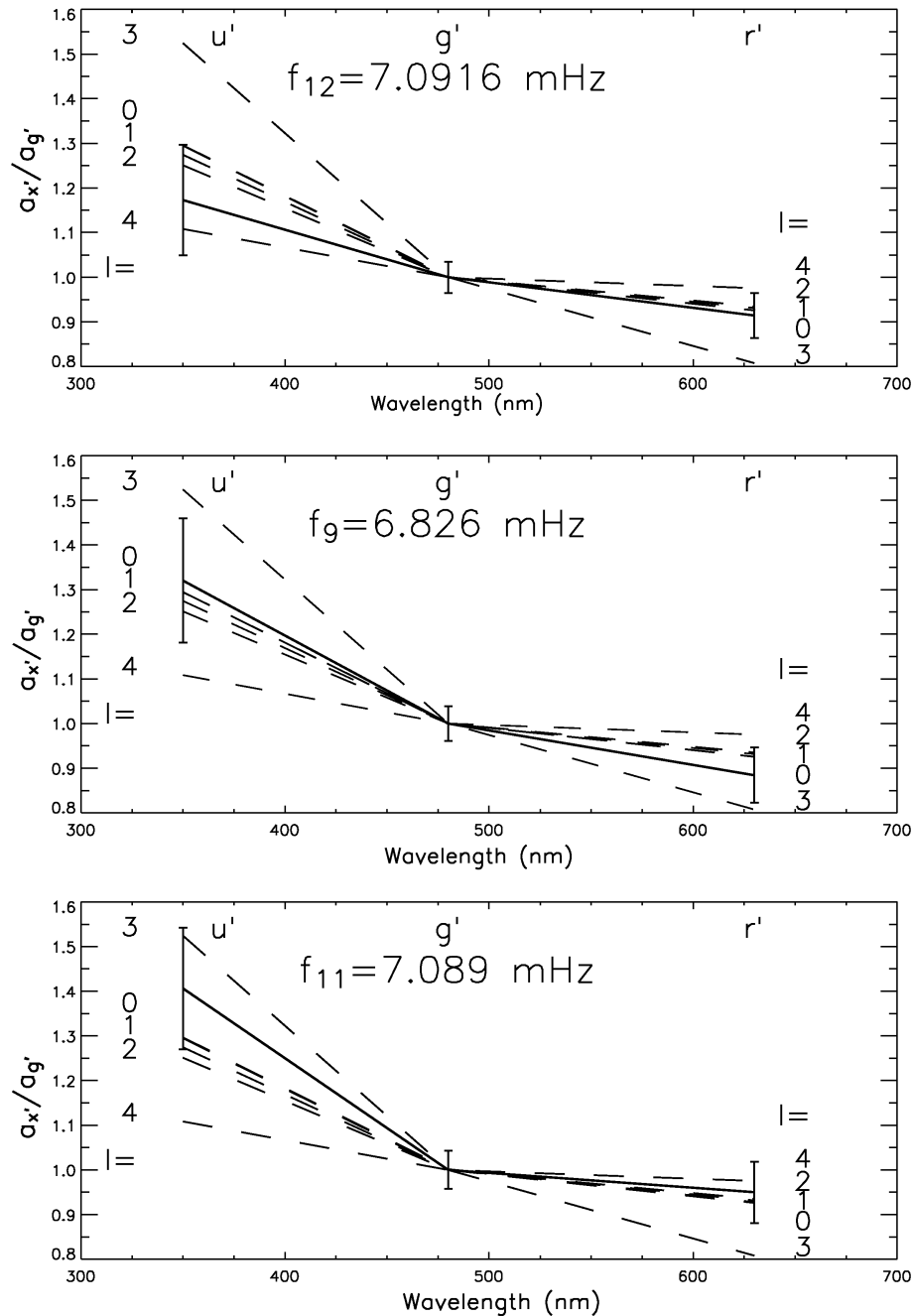


**Fig. 10.** Amplitude ratios for the three largest amplitude modes in PG 0014+067 (solid) and from theory (Ramachandran et al. 2004, dashed lines). From Jeffery et al. (2005).

Hawaiian island of Maui.  $\sim 8$  hours data obtained over five nights proved invaluable for improving the window function and enabling us to identify 19 frequencies correctly.

Two segments of the “white light” curve, obtained by combining the 3-channel ULTRACAM data with data from the Faulkes telescope, together with the 19-frequency solution, are shown in Figure 8. One important goal was to verify

previous frequency analyses (Figure 9). Most major frequencies identified previously were confirmed, differences are probably due to cycle  $d^{-1}$  aliases.

In terms of mode identification, the results were less conclusive than for the targets observed in 2004. However it was possible to show that the two dominant modes must be  $\ell = 0, 1$  or  $2$  (Figure 10), and to find evidence that the rotational period should be nearer to 4 d than to the 1.35 d reported previously. The first result is significant because it contradicts the best seismic models (Charpinet et al. 2005, Brassard et al. 2001), in which the dominant mode has  $\ell = 3$ .

Full details of this analysis have been published by Jeffery et al. (2005). Preliminary results of the 2004 WET campaign on PG 0014+067 are presented by Kawaler et al. (2006).

## 5. THE FUTURE

ULTRACAM has proved to be a powerful instrument for the interpretation of, to date, four pulsating sdB stars. There are three ways in which it will make a significant impact in the future. Mounted on an 8 m class telescope, such as the VLT, it can provide outstanding multicolor light curves for short-duration events, such as eclipses in those HW Vir systems which contain a pulsating sdB star. In conjunction with other 4 m telescopes, multi-site campaigns covering four to seven days and multicolor photometry of stars brighter than 15th mag. will allow identification of both frequencies and  $\ell$  values for modes with amplitudes 0.5 mmag or less. Finally, the prospect that ULTRACAM may be available for more extended periods on a 2.5 m class telescope offers the prospect of extending mode identifications to a much larger sample of sdBVs than has been possible so far.

## REFERENCES

- Aerts C., Jeffery C. S., Dhillon V. S. et al. 2006, *Baltic Astronomy*, 15, 275 (these proceedings)
- Brassard P., Fontaine G., Billères et al., 2001, *ApJ*, 563, 1013
- Charpinet S., Fontaine G., Brassard P., Dorman B. 2002, *ApJS*, 140, 469
- Dhillon V., Marsh T. R. 2001, *New Astr. Rev.*, 45, 91
- Fukugita M., Ichikawa T., Gunn J. E., Doi M. 1996, *AJ*, 111, 1748
- Heynderickx D., Waelkens C., Smeyers P. 1994, *A&AS*, 105, 447
- Jeffery C. S., Dhillon V. S., Marsh T. R., Ramachandran B. 2004, *MNRAS*, 352, 699
- Jeffery C. S., Aerts C., Dhillon V. S., Marsh T. R., Gänsicke B. 2005, *MNRAS*, 362, 66
- Kawaler S. 2006, *Baltic Astronomy*, 15, 283 (these proceedings)
- Koen C. 1998, *MNRAS*, 300, 567
- Ramachandran B., Jeffery C. S., Townsend R. H. D. 2004, *A&A*, 428, 209
- Townsend R. H. D. 1997, Ph. D. Thesis, University College London